CREATING A LOW-NOISE, ULTRAFAST OPTICAL NONLINEAR SHUTTER BASED ON THE KERR EFFECT

by

DAVID LEFÈVRE

A THESIS

Presented to the Department of Physics
and the Robert D. Clark Honors College
in partial fulfillment of the requirements for the degree of
Bachelor of Science

May 2024

An Abstract of the Thesis of

David Lefèvre for the degree of Bachelor of Science
in the Department of Physics to be taken June 2024

Title: Creating a Low-Noise, Ultrafast Kerr Optical Nonlinear Shutter Based on the Kerr Effect

Approved: *Brian Smith Ph.D.*
Primary Thesis Advisor

Experiments on entangled photon pairs and astronomical interference require an ultrafast shutter that can isolate desired photon pulses. The Kerr-effect in third order nonlinear optics has been used to create a shutter that operates on the femtosecond timescale. Low noise Kerr-effect shutters capable of completing single photon pair experiments have been created using high pump filtering and high signal transmission.[1,2] Unlike other low noise shutters, measurements of Raman scattering from the pump pulses are collected. Another unique feature of this Kerr-Effect shutter is that it uses signal and pump wavelengths, 1550nm and 850nm, respectively, that have not been tested in previous research. Unfortunately, the Raman scattering measurements must be retaken due to potential errors with the pump beam being continuous wavelength instead of pulsed. Transmitted signal power was measured in relation to pump power and pump polarization angle, both of which indicated the possible presence of the Keff effect. Our Kerr shutter managed to isolate 31.9% of the expected power.

Acknowledgements

I would like to thank my primary thesis advisor, Brian Smith, for helping provide me with context, direction, and opportunity to complete this research. Matt Brown has also been of great help throughout this process by teaching me the ins and outs of this optics research as well as challenging me to slow down and think like a scientist. I would also like to thank the Mentored Research Program for providing funding for my research. Finally, I would like to extend thanks to my friends, teachers, and peers who have supported me throughout this project.

Table of Contents

List of Figures

List of Tables

BACKGROUND

To avoid being blurry, a photograph must be taken faster than the object being captured moves. Shutters have been used and improved for the last 150 years to take photos and videos as well as advance photonics. They work by isolating a segment of light (typically in time) to be absorbed by a sensor. Higher shutter speeds allow for finer time dependent dynamics to be captured. Thomas Skaife took pictures of cannon balls in flight at Woolwich Arsenal in 1858 using two half doors held together with elastic bands to have a 20ms second shutter.[3,4] Similarly, Eadweard Muybridge sequentially triggered cameras with a revolving disc shutter with 1ms shutter speed to capture a moving horse in 1878.[3,5] Sophisticated mechanical shutters reach their inherit limit with 0.4 microseconds shutter speeds.[3] Beyond their use in digital cameras, shutters are necessary for experimental groups imaging cutting-edge physical phenomenon. Electro-optical shutters are the next quickest, cracking into the nanosecond timescale.[2] To expand beyond the limitations of electronics, ultrafast all-optical techniques have been developed, such as the Kerr shutter.[4,6,7] Further advances have been made to create attosecond laser pulse that can image electrodynamics, a feat which was awarded the 2023 Nobel prize in Physics.[6]

Maxwell's equations are the fundamental laws governing electromagnetism,

$$\nabla \cdot D = \rho_f \ , \quad \nabla \times E = -\frac{\partial B}{\partial t} \ , \qquad \nabla \cdot B = 0 \text{ , and } \qquad \nabla \times H = \frac{\partial D}{\partial t} + J,$$

with D being the electric flux density, E being the electric field vector, ρ_f being the charge density, B being the magnetic flux density, H being the magnetic field vector, and J being the current density. A wave ψ must satisfy the wave equation $\nabla^2\psi = \frac{1}{v^2}\frac{\partial^2\psi}{\partial^2 t}$, where v is the velocity. Electromagnetic radiation, commonly referred to as light, is a unique phenomenon derived from Maxwell's equations that fits the form of a wave equation by having its electric and magnetic fields perpendicular to each other and to the direction of its propagation. As a result, the

magnetic field can be found assuming the electric field direction, called polarization, and travel direction are already known. The wave equation reveals that light propagates through space at a constant speed, aptly named the speed of light, and oscillates with varying possible wavelengths. While observable light is a narrow range of wavelengths(380-700nm) that human photoreceptor cells can absorb, light can have wavelengths ranging from long radio waves to short gamma rays.[8]

Since light's direction of motion is perpendicular to the electric field and the polarization is parallel to the electric field, polarization must be normal to the direction of travel. Polarization is described by its two oscillating components within its plane, which can be mathematically written using Jones matrices,

$$J = \begin{bmatrix} A_x \\ A_y \end{bmatrix} = \begin{bmatrix} a_x e^{i\varphi_x} \\ a_y e^{i\varphi_y} \end{bmatrix} \quad .[9]$$

Light is described as linearly polarized when the polarization components have a phase factor of π between their oscillations. Otherwise, light is described as having elliptical polarization when $\Delta\varphi = \varphi_x - \varphi_y \neq n\pi$, where n is any integer. Importantly, the Jones vectors can be acted upon by optical components that are mathematically expressed as Jones matrices. Linear polarizers only transmit the component of polarized light aligned with the transmission axis and have Jones matrix $T = \begin{bmatrix} 1 & 0 \\ 0 & 0 \end{bmatrix}$ for transmission of the X axis polarization. Wave retarders add a phase along one axis within the polarization plane which transforms linear to elliptical polarization in a quarter waveplate(QWP) and rotates the polarization 90° in a half waveplate (HWP). The Jones vector for a wave retarder is $T = \begin{bmatrix} 1 & 0 \\ 0 & e^{-i\tau} \end{bmatrix}$.[9]

Light has important properties when interacting with materials. While light in vacuum travels at the speed of light, light in a medium is slowed by a factor of the inverse of the

refractive index of a material (n>0). Materials' refractive index is determined by how it interacts with applied electric and magnetic fields. Materials react to an exterior electric field (E) and magnetic flux density (B) with their polarization (P) or magnetization (M), respectively. This interaction is used to define the electric flux density(D) and magnetic field(H), as shown below

$$D \equiv \epsilon_0 E + P \quad \text{and} \quad H \equiv \frac{1}{\mu_0} B - M \quad .[10]$$

These phenomena are created by shifting the bound electrons atoms within a material to have electric polarization by being offset with respect to nuclei or magnetism with spin alignment. Linear materials are defined by having the induced polarization linearly dependent on the electric field ($P = \chi_e E$) and magnetization linearly dependent on the magnetic field ($M = \chi_m H$).[10] Linearity allows for the following simplification by introducing permittivity (ϵ) and permeability (μ) defined below

$$\epsilon = \epsilon_0(1 + \chi_e) \quad \text{and} \quad \mu = \mu_0(1 + \chi_m) \; .[10]$$

μ_0 is the permeability of free space and ϵ_0 is the permittivity of free space. This simplifies the electric flux density and magnetic flux density to be

$$D \equiv \epsilon E \quad \text{and} \quad B \equiv \mu H \; .[10]$$

A materials index of refraction(n) is defined using ratios of the permittivity (ϵ), permittivity of free space (ϵ_0), permeability (μ), and permeability of free space (μ_0)

$$n = \sqrt{\frac{\epsilon\mu}{\epsilon_0\mu_0}} = \sqrt{(1 + x_e)(1 + x_m)} \quad .[10]$$

At the boundary between two mediums that have different refractive indexes, light can be refracted and reflected. Refraction follows Snell's law ($n_1 \sin(\alpha_1) = n_2 \sin(\alpha_2)$). Snell's law implicitly follows the ray model of light describes rays that travel through media with a set of geometric rules.[9] When traveling from a higher to lower refractive index medium, there's a

critical angle at which the equation breaks down. At or past the critical angle, mediums have total internal reflection where all light is reflected and none is refracted.[9] Fiber optics have a cylindrical core that has a higher index of refraction than the cladding material that surrounds it. The ray model uses total internal reflection to describe how light propagates through the core. For propagation, light must enter the optical fiber within an acceptance angle $\theta_a = \sin^{-1} NA$, where the Numerical Aperture (NA) is given by $NA = \sqrt{n_1^2 - n_2^2}$.[9] The wave model of light begins by solving the wave equation with appropriate boundary conditions and finding fiber modes that guide the propagating light. These guided modes are characterized by the number of azimuthal and radial nodes in their transverse intensity distribution. The wave description of electromagnetic radiation is compatible with the ray particle view of total internal reflection by having wave equations with exponential decrease in the cladding. The number of allowed guided modes is related to a parameter (called the V parameter), $V = 2\pi \frac{a}{\lambda_0} NA$, which is determined by the wavelength of the light propagating in the fiber(λ_0), core diameter(a), and NA. Optical fibers are often characterized as single mode or multimode. Different guided modes have different propagation speeds, which results in modal dispersion for propagation in multimode fibers. Dispersion is the lengthening of pulses as they travel through a medium.

Additionally, the refractive index of mediums varies depending on the wavelength of light, which causes the different wavelengths to spread apart due to having different velocities. Two different light frequencies entering a medium at an angle will be refracted to different angles according to Snell's law. Spectrometers rely on this phenomenon to separate and detect different wavelengths at different spatial positions. A medium whose refractive index is dependent on the polarization and direction of propagation is described as having birefringence. It was not until the invention of the laser in the 1960s that physicists had sufficient light intensity

to study the nonlinear behavior of mediums.[9] Nonlinear mediums are characterized by having a polarization density with a nonlinear dependence, such as quadratic or cubic, on their electric field.

$$P = \epsilon_0 \chi E + \chi^{(2)} E^2 + \chi^{(3)} E^3 + \cdots \quad .^{9}$$

Second order nonlinear optics have a quadratic dependency and allow for the addition and difference between two frequencies of light to generate a third frequency, called up conversion and down conversion, respectively. Additionally, a parametric amplifier splits a segment of a powerful initial light beam into two smaller frequencies.[9] The high intensity beam input for many of these devices is called the pump and the signal is the desired output beam, which is sometimes an input that is altered or amplified.

Third order nonlinear mediums that have a cubic nonlinear dependency that dominates other terms are called Kerr mediums. These mediums exhibit the optical Kerr effect, which is where the refractive index is linearly dependent on the electric field intensity in the electric field's axis

$$n(I) = n_0 + n_2 I \quad .^{9,11}$$

In this equation, n_0 is the original material index of refraction and n_2 is the optical Kerr coefficient that is dependent on wavelength. One such effect of the optical Kerr effect is cross-phase modulation, where pump light going through a third order nonlinear medium creates birefringence along its polarization axis and hence a phase shift to the signal light. Thus, when the signal and pump light overlap as they travel through a third order nonlinear medium, the signal light behaves as if it were going through a waveplate.

By utilizing the polarization rotation of the signal by optical Kerr effect, one can separate a segment of the signal in time creating a shutter that does not require mechanical or electrical

means. This Kerr effect shutter is maximized by the signal and pump laser having (1) paired staggered pulse emission, (2) linear polarization with 45° offset, (3) optical paths that allow overlap in the fiber, (4) increased coupling into the optical fiber, (5) spatial overlap within the fiber, as well as (6) the ability to filter out the pump and the other polarization basis vector of the signal pulse. Group velocity dispersion between the signal and pump pulse allow the pulses to propagate through each other ensuring that the entirety of the signal pulse gains a phase from the induced birefringence. Besides temporal overlap of the pump and signal, spatial overlap of the pulses ensures that process is as efficient as possible. The signal pulse experiences a lack of rotation when the pump is absent. One segment of the signal field has changed polarization with respect to the rest of the field as the signal field exits the optical fiber, which allows for selection of different parts of the field by polarization. The Kerr Effect induced phase shift of an optical pulse with a Gaussian beam shape is

$$\theta_1(T) = \sqrt{\pi}\gamma P L_w[\mathrm{erf}\left(\frac{T}{T_0}\right) - \mathrm{erf}\,(\frac{T}{T_0} - \frac{L}{L_w})] \,,$$

where $L_w = \frac{T_0}{d_w}$, $d_w = \frac{1}{v_{g1}} - \frac{1}{v_{g2}}$, and $\gamma = \frac{2\pi n_2}{\lambda A}$.[12] Additionally, P is the peak power, erf is the error function, L is the fiber length, v is the group velocity of different pulses, A is the fiber area, n_2 is the Kerr constant, T_0 is the pump pulse time, T is the time, and λ is the signal pulse center wavelength. The waveplate phase is linearly proportional to power, so the equation can be written as $\theta = aP$ where a is a constant from the signal, pump, and fiber physical properties.

Once the signal pulse switches from vertical to horizontal polarization, a polarized beam splitter (PBS) can isolate the horizontal from vertical polarization. These shutters have been utilized in classical optics for several decades and have recently been utilized for single photon shuttering.[1,2,13]. The transmissivity (T_s) is the percentage of signal laser power transmitted through a PBS after having its polarization rotated from the Kerr effect. The transmissivity

is derived using Jones polarization vectors and matrices. The transmissivity is simplified as the signal light undergoing the Kerr effect (which is the same as going through a phase retarder) and PBS. Let's set the x/y plane with respect to the pump pulse such that $T_R = \begin{bmatrix} 1 & 0 \\ 0 & e^{-i\theta} \end{bmatrix}$. From there redefine the linear polarization of the signal with respect to the new axes such that $J_o = \begin{bmatrix} \cos\alpha \\ \sin\alpha \end{bmatrix} \varphi_0$ where $1 = |\varphi_0|^2$. The PBS transmission polarization is 90° rotated with respect to the initial signal linear polarization such that $J_{90P} = \begin{bmatrix} -\sin\alpha \\ \cos\alpha \end{bmatrix} \varphi_0$. The transmission is derived below.

$$T_s = |J_{90P}{}^* * T_R * J_o|^2$$

$$T_s = \sin(2\alpha)^2 \sin(\frac{\theta}{2})^2$$

The transmission can have the phase written as a function of power using the previously mentioned equation $\theta = aP$.

$$T_s = \sin(2\alpha)^2 \sin(\frac{aP}{2})^2$$

Now the transmission is a function of power and relative signal and pulse angle. Both of these are measurable and can be experimentally tested.

Figure 1 is a plot of the transmission as a function of Power with the relative polarization angle maximized.

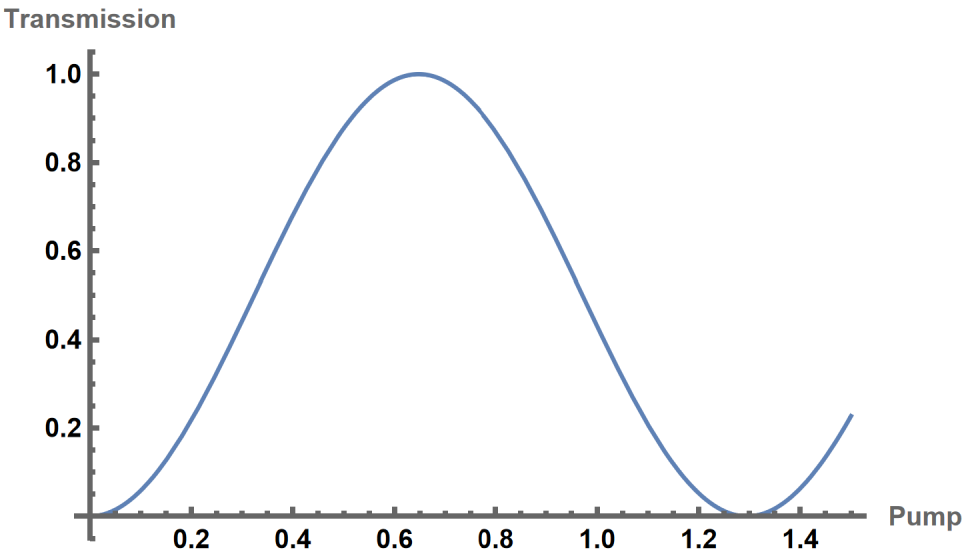

Figure 1: Transmission Signal Power vs. Pump Power(mW)

Plot of transmission equation as a function of phase nested with phase as a function of power.

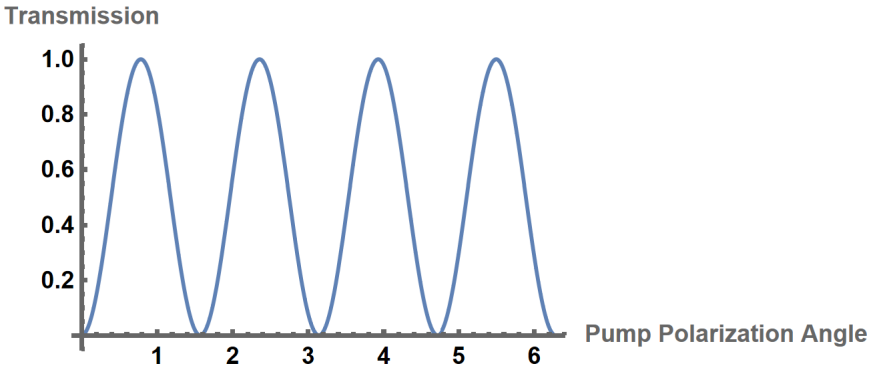

Figure 2: Signal Power Transmission vs. Pump Polarization Angle (Radians)

Figure 2 is a plot of transmission as a function of the relative polarization angle while setting the power such that the phase shift is $\theta = \pi$. Putting a lot of energy into materials to observe nonlinear effects makes it difficult to make low noise measurements. Mediums' lattices have atomic wave vibrations called phonons. At high energy, pulses of light can transfer energy to or from vibrational modes of the system, which is called Raman scattering.[14–16] Raman Gain occurs in third order nonlinear mediums, which can serve as an experimental challenge by adding energy to the 1550nm signal field. Additional energy transferred to a signal field could be

detrimental to single photon experiments and must be measured to determine the extent of the additional noise it creates.

Experiments on entangled photon pairs and astronomical interference require an ultrafast shutter that can isolate desired photon pulses. Low noise Kerr-effect shutters capable of completing single photon pair experiments have been created by having high pump filtering and high signal transmission.[1,2] The unique feature of this Kerr-Effect shutter is that it uses different signal and pump wavelengths, 1550nm and 850nm, respectively, compared to previous research. Possible issues caused by Raman scattering from the 850nm pump pulse will be monitored. This research aims to build a Kerr Effect shutter that can be used for astronomical interferometry and single photon quantum optics projects within the Smith laboratory at the University of Oregon.

RESEARCH QUESTIONS

1. How can a Kerr-Effect Shutter with a 1550nm signal pulse and 850nm pump pulse be created to isolate two signal pulses separated by 200 picoseconds?

2. What impact will Raman Scattering from the pump pulse have on the signal pulse exiting the shutter?

3. Can the shutter be adjusted to function with single 1550nm photon pulses?

METHODS

General Setup

Building a Kerr effect shutter requires controlling the power, relative polarization, and relative timing of the signal and pump pulse. Beam profiling describes the beam expansion through the optical path. Fiber coupling is important to maximize power needed for the Kerr effect. Beam timing was controlled through rough optical path length measurements during initial set up as well as optical path length adjustments using a path delay arm in the pump path when measuring the relative pulse timing with a IQ Quantique 1000 time tagger. Polarization was controlled using quarter and HWPs as well as PBS. The Kerr Effect was tested by adjusting the pump power and polarization as independent variables and having signal pulse transmission through a PBS as the dependent variable. Building a low noise Kerr Effect shutter was worked towards by measuring the Raman scattering using superconducting nanowire single photo detectors and filters. Figures 3 and 4 show the experimental apparatus used.

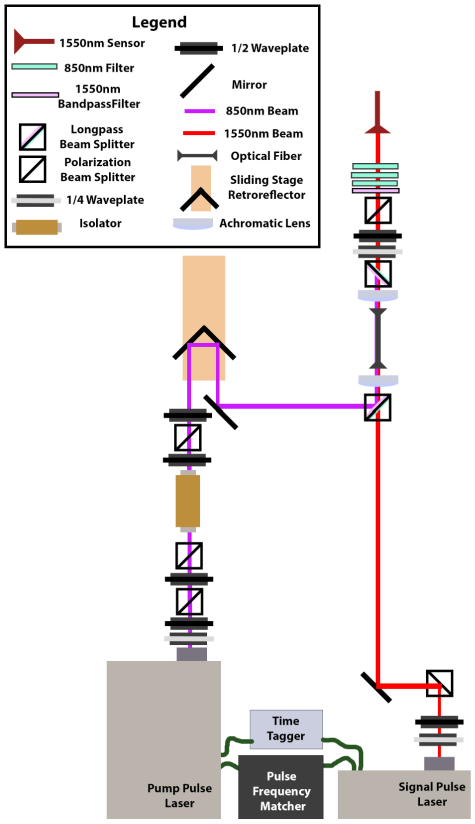

Figure 3: Diagram of Adjusted Experiment Apparatus

From the initial to final setup, the pump optical path gained an isolator, PBS, and HWP. Labels of optical components are in Legend.

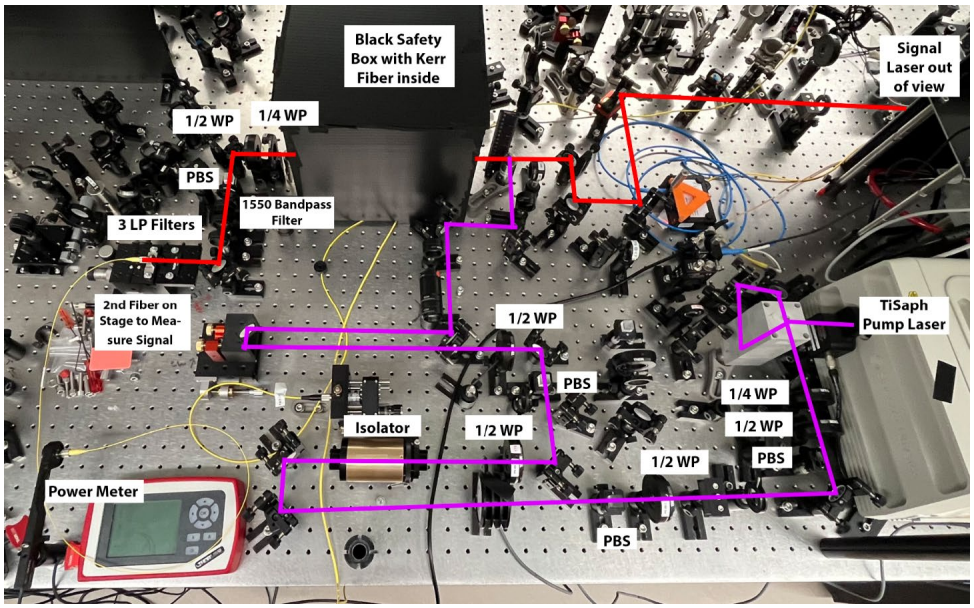

Figure 4: Photo of Adjusted Experiment Apparatus

Pulse Timing

Now the pump pulse path length must be adjusted such that it overlaps with the signal pulse in the kerr fiber. Preliminary calculations show that for the timing to overlap within the 10cm optical fiber the two pulses must be within a fraction of a millimeter of each other, which is an obtainable accuracy. Prelimary calculation for 1m fiber and an 850 as well as 1550nm light pulses indicate that a spatial seperation of around a millimeter is sufficient to ensure full crossover within the fiber as a result of its dispersive properties. A few steps must be taken to have pulses overlap within the Kerr fiber. Firstly, the optical path lengths of the signal and pump pulse were measured with a ruler to be equalized within two inches. Secondly, the signal laser, pump laser, and ID Quantique 1000 time taggers were set up so that a trigger system could nearly simultaneously record the release of the pump and signal pulse as well as record their relative arrival times. Thirdly, the pump pulse must be checked to still couple at varying retroreflector distances. Fourthly, adjust the retroreflector mirror to equalize the relative pump and signal travel distance.

The second step must be elaborated on to be better understood. The Origami laser simultaneously emitts a laser pulse as well as an electrical signal that is split and sent to both the Ti:Sapphire(Ti:Sa) laser as well as the time tagger. The Origami laser has a pulse frequency of approximately 80Mhz. Each time a light and electrical pulse is sent out, the electrical signal starts an internal time counter upon arrival to the time tagger. Once the light pulse arrives at the Multi-Photon Device (MPD), it is transformed into an electronic signal that travels to the time tagger machine and ends the time counter upon arrival. The electronic pulse sent to the Ti:Sa is transformed into an optical pulse and then at the MPD is transformed back into an electornic pusle sent to the time tagger. The pump pulse timing can be determined only once the two lasers

are frequency locked together ensuring that when a pulse is emitted from the origami another pulse from the Ti:Sa. Frequency locking was fairly temperature sensitive and would not lock if the laboratory was a degree or two outside the standard range.

The MPD is a sensitive photodetector that resolves down to the single photon level. As a result, the photodetector has a maximum threshold of roughly 300,000 photon counts per second or $2.34 * 10^{-15}W$ for 850nm wavelength. Pulse power was lowered to an acceptable range using the quarter and HWPs as well as Neutral Density (ND) filters with a total optical density of 15. Procedurally, the pulse power was turned up to around 50mW and then ND filters were used until the Thorlabs detector read zero. From there the ND filters were kept and the WP angles were returned to minimize the initial pulse power before the ND filters from 50mW to <1 μW. Experimentally only ND 12 was required for the Pump pulse to have around 1,000 photon counts per second. The signal pulse is at 1550nm wavelength, which is not directly absorbed by the MPD. Thus, much larger powers were sent into the detector to detect the signal pulse, since a count is only made via two photon absorption where two photons nearly simultaneously excite an electron to create a signal. A signal pulse around $7\mu W$ was experimentally found to lower the signal pulse into an acceptable power range for MPD detection. The MPD was connected to the end of the Kerr fiber for detection. To prevent high backgorund counts, lights in the laboratory were turned off.

In cases where the light pulse travels a significantly longer distance than the electronic pulse, the next electronic pulse sent out from the Origami arrives before the light pulse ends the time tagger. This results in the time tagger to start from zero again, which is important to understand the relative timing between the pump and signal pulses found experimentally in figure 5, 6, and 7. In thse figures, the signal pulse pulse can be identified as

the narrow pulse since it is single mode in the Kerr fiber. The pump pulse is wider than the signal pulse since it is multimode in the Kerr fiber. Different modes travels at different speeds, so the multimode pulse spreads out as it travels through the fiber.

Table 1 shows that the initial relative time difference was 2.315ns, which corresponds to 27.38 inches of extra distance required for the pump pulse to be within the range of the signal pulse. Additional mirrors were added to increase the pump pulse's optical path length by 26 inches, which is shown by the shift between figure 6 and 7. Adjusting the retroreflector distance then further lowered the relative timing differences between the two pulses, which is shown by the shift between figure 6 and 7. Figures 6 and 7 are screen shots. The relative timings are determined by timing the signal and pump pulses seperatelys.

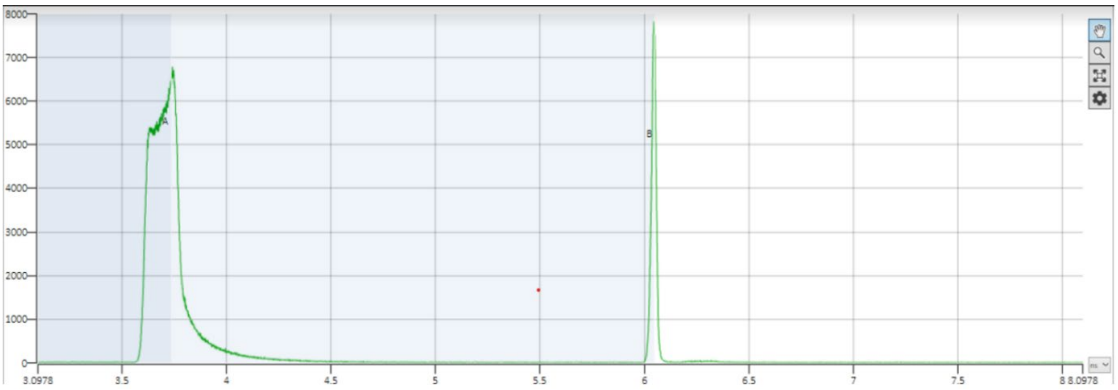

Figure 5: Initial Photon Count vs. Time(ns) for Signal and Pump Pulses

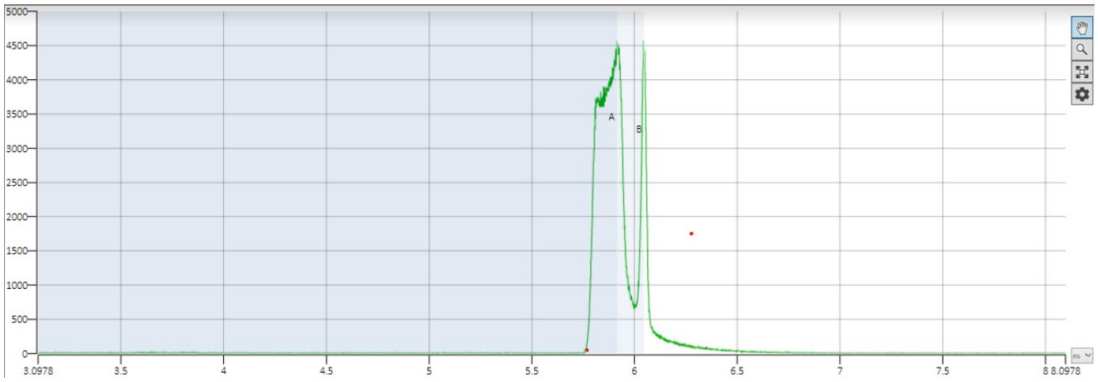

Figure 6: Photon Count vs. Time(ns) for Signal and Pump Pulses after 1st Adjustment of Pulse Beam Path

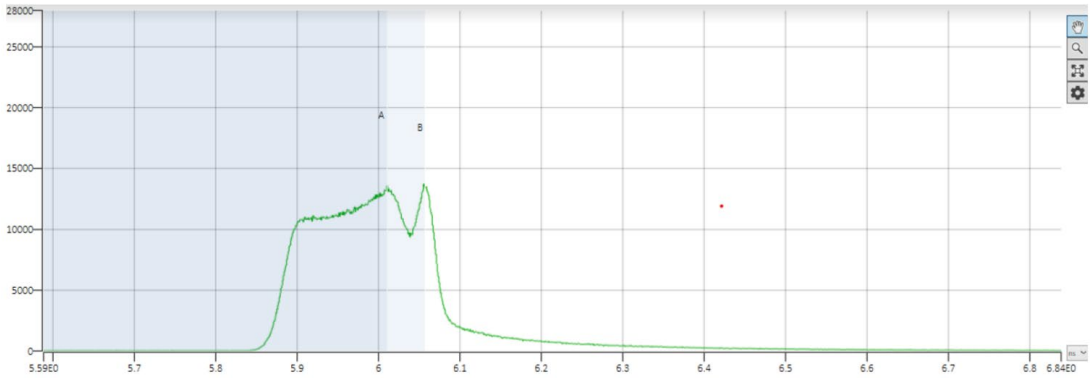

Figure 7: Photon Count vs. Time(ns) for Signal and Pump Pulses after 2nd Adjustment using Retroreflector Position on Stage

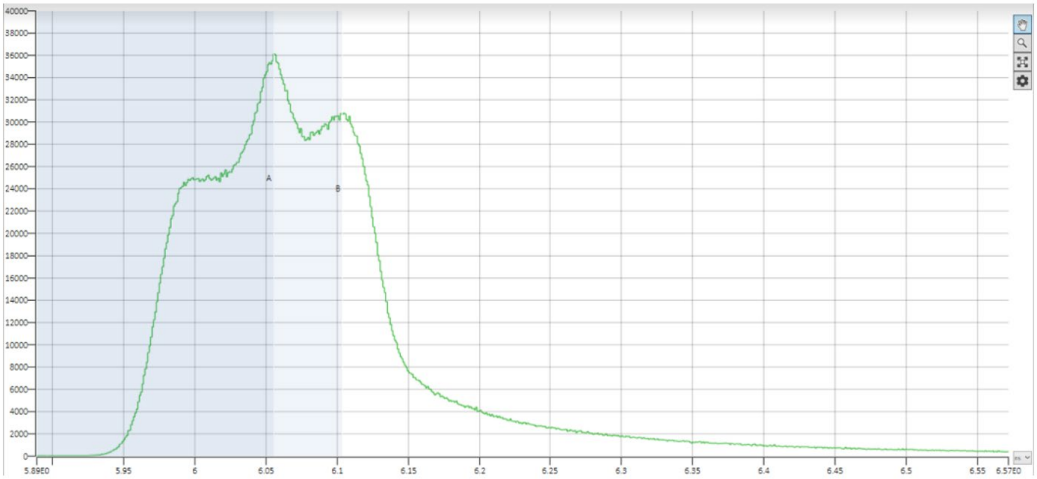

Figure 8: Photon Count vs. Time(ns) for Signal and Pump Pulses after Adding Insulator

Iteration	Pump Time(ns)	Signal Time(ns)	Relative Difference (ns)
1	3.732	6.047	2.315
2	5.916	6.047	0.131
3	6.01	6.057	0.047
4	6.103	6.055	0.048

Table 1: Relative Timing of 4 Iterations of Signal and Pump Pulses

By the 4th iteration, the pump and signal pulse had enough temporal overlap to begin testing for the Kerr Effect. In trying to find the effect, it was noticed that the pump pulse was not mode-locking properly. It was determined via process of elimination using a beam blocker that the pump laser was unable to mode-lock as a result of laser back reflection from the Kerr fiber coupling area. To remove this issue an optical isolator, which is a unidirectional optical filter, was placed within the beam path. The different index of refraction within the isolator along with retroreflector adjustments allowed for the overlap shown in figure 8. Adjustment of optical path lengths via mirror changes as well as retroreflector adjustment is paired with time tagging to have adequate temporal overlap between the signal and pump pulse.

Controlling Polarization

A PBS transmits horizontally polarized light and reflects vertically polarized light. Horizontal light transmission has less leakage from other polarizations than of vertical light reflection, so the signal pulse is vertically polarized before entering the kerr fiber by a PBS. Place a power detector to verify the minimization of transmitted light power through the PBS. With the signal vertically polarized, the measured power transmitted through the PBS is the background count for measuring the Kerr Effect. From there, turning on the pump pulse should result in the Kerr switching to take place, which will rotate the signal pulse polarization (from vertical to horizontal polarization) and allow for a significantly larger portion of the light to be transmitted and meausred by the power meter. Additionally, QWPs and HWPs are placed after the Kerr fiber to negate the any birefringence effects due to stress on the fiber. Unfortunately, the signal pulse was reflected off of the corner of a mirror, which likely resulted in additional polarization phase shift. Table 2 shows that increasing power resulted in lowering the percent of

out of phase light while still increasing the total transmitted power. To minimize the percentage of non-vertical light, the total signal pulse power is increased.

The pump pulse polarization is initially horizontal due to horizontal transmission throguh the PBS. It is then is lowered via the 45° isolator polarizer, and it is lastly rotated to a desired degree with the HWP placed after the isolator. The HWP placed after the isolator is initially set to be 45° between the maximum and minimum angle of light power transmission through a temporary PBS measured by a Throabs powermeter through a temportant. Being 45° off from the signal pulse's vertical polarization is important to be near the maximum degree to observe the Kerr effect. Maximum power was found at 94° and mimumum power was found at 135°, so the HWP was rotated to the midway angle of 115°.

Power Before PBS (μW)	Power After PBS (mW)	Transmission (%)
155.7	0.355	43.9
180.0	0.990	18.2
218.4	27.7	0.79

Table 2: Percent of Signal Pulse Horizontally Polarized by Power

The signal pulse was coupled into the Kerr fiber with 42.9% efficiency and the second fiber was coupled with 50.6% efficiency. The signal pulse power was increased such that the second fiber was reading around 7mW. The angles of the QWP and HWP placed after the Kerr fiber were adjusted to minimize the power reading, resulting in the power reading in the 2nd fiber to lower from 7mW to 5.20 μW. Thus, the polarization through the Kerr fiber was minimized such that the signal pulse is vertically polarized within a small degree of error.

Raman Scattering

A major consideration within this research is the question of how many 1550nm photons are created via Raman scattering from the higher power 850nm beam in the Kerr fiber. To measure 1550nm light on the single photon scale, superconducting nanowires were utilized. Given the high sensitivity of the superconducting nanowires, a power meter with nanowatt sensitivity was connected to the collector fiber and checked to read no power from either the background or pump light going through the Kerr fiber. From there a 950nm onset long pass beamsplitter (<1% 850nm transmission), three 1200nm long pass filters ($\sim 0.01\%\ 850nm$ transmission). After this power meter zeroing check, measurements were made on the of the background light using the superconducting nanowire sensors. From there, the 850 nm beam was turned on with d=15 ND filters blocking any light transmittance and slowly removed to lower risk of damaging the sensitive nanowires (>1 million photons could cause damage). Eventually all ND filters were removed and Raman scattering counts were detected. Since the filters mentioned above only block frequencies >1200nm, a 1560nm bandpass filter with a 12nm Full Width Half Max (FWHM) was added to eliminate Raman scattering detection from frequencies above 1200nm outside of the bandpass range. The bandpass filter was found to transmit 60.4% of the 1550nm laser and ~0.1% of the 850nm laser. Figure 9 depicts a black box placed over the Kerr fiber during this process as a safety mechanism against the leaking 850nm light from the Kerr fiber as seen in figure 21. This safety feature is important given that the 850nm laser power is increased to several hundred milliwatts and has a low coupling efficiency. When measuring the Raman scattering, the 850nm laser has roughly 51-55% coupling efficiency into the Kerr fiber and the 1550nm laser had an 83% coupling efficiency from exiting the Kerr fiber to entering the light sensor.

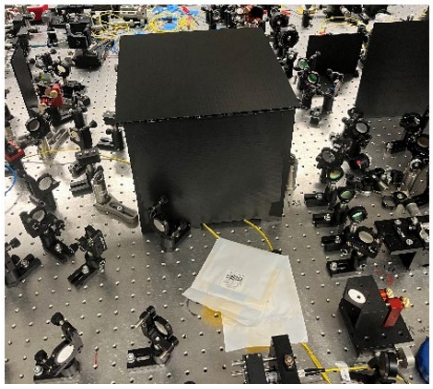

Figure 9: Black Box Over Kerr Fiber

ANALYSIS

Kerr Effect

With the pump and signal pulse overlapping in the kerr fiber, the initial kerr shutter abilities can be verified. An initial check to ensure that the Kerr effect may be present is to have the signal pulse on and then switch the pump pulse on and observe an increase in power. The second part of this initial check is to keep the pump pulse on and switch the signal pulse off and observe the power meter read zero. This initial check was completed first before proceding to measure more senstive features of the Kerr effect. After noticing this initial test, the retroreflector was adjusted to maximize the noticed change in power from the Kerr effect. For sensitive tests of the Kerr Effect, two parameters can be adjusted: pump pulse angle and pump pulsepower. The pump pulse angle can confirm the existence of the Kerr effect by checking that a 45° difference between the initially horizontal signal pulse and pump pulse maximizes the Kerr effect. Plot the transmitted power versus the pump pulse angle with respect to the horizontal plane. A sinusoidal squared with a maximum value at 45° is expected.

Rotating the pump pulse HWP roughly followed the sinusoidal pattern expected, but on a much tighter range of angles than expected. Instead of repeating the sinuisoidal pattern every ninety degrees, fitting a sinusoidal squared to figure 11 shows that one wavelength is around 11.7°. With this level of rapid fluctuation, plotting transmitted signal pulse power for every 5° in the whole 360° lacks resolution, as shown in figure 10. Figures 10 and 11 were both measured with 770mW of pump power.

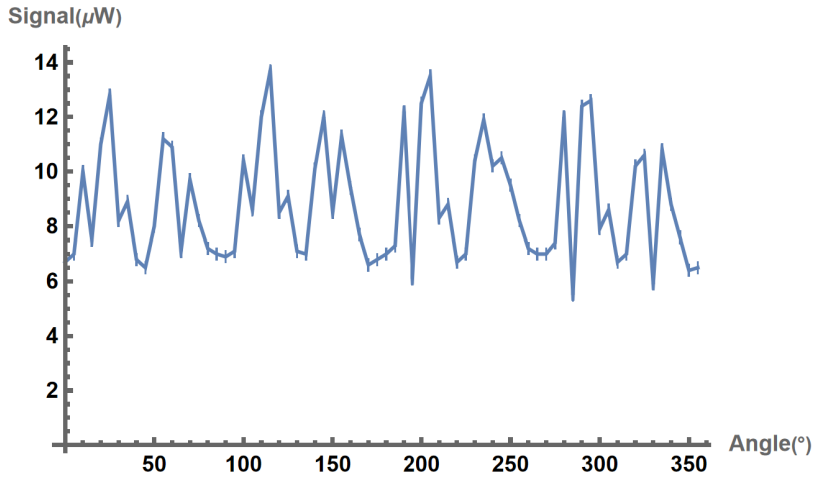

Figure 10: Signal Pulse Power (μW) vs. Pump HWP Angle (°)

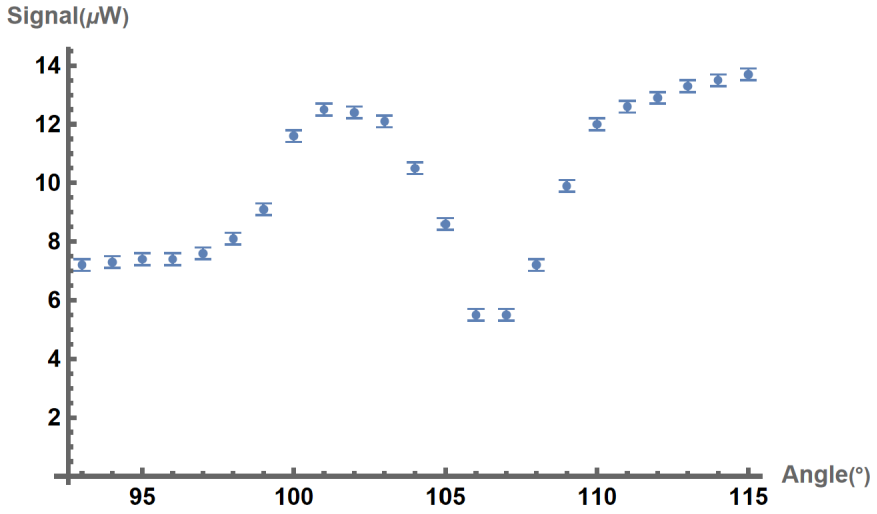

Figure 11: Signal Pulse Power(μW) vs. Pump HWP Angle (°)

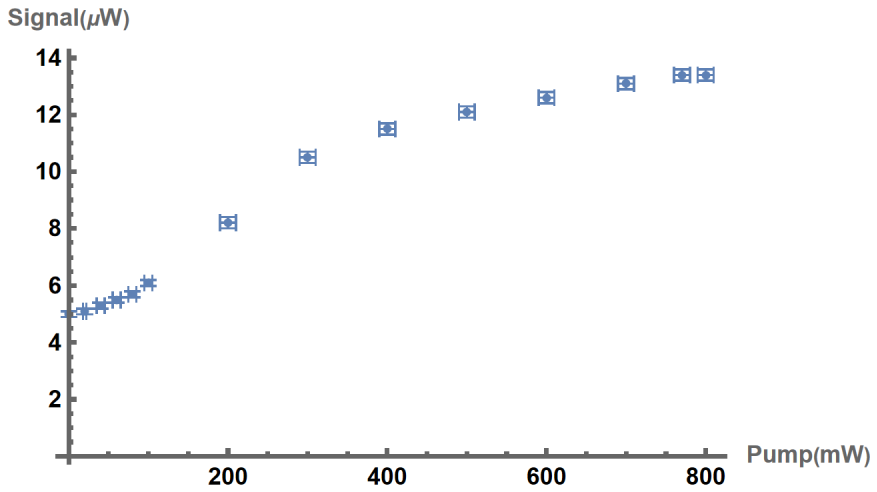

Figure 12: Signal Pulse Power(μW) vs. Pump Pulse Power(mW)

The pump pulse power coupling efficiency was 45% for figures 10, 11, and 12 and 42% for figures 13 and 14. In figures 12, 14, and 15, the x axis has the total pump power, not the amount coupled into the Kerr fiber. The transmitted signal power should vary due to the pump HWP angle accordign to the equation, $T = \sin(2\theta)^2$, which predicts 4 peaks over 360°. Figure 15 has around 8 clumps of peaks instead of the expected 4. Thinking that the pump pulse polarization was possibly the reason for the inconsistency with angular rotation, a PBS was added after the insulator and before the HWP to remove any elliptical polarization generated within the isolator. Additionally, a HWP was added before the PBS to rotate the beam coming out of the isolator at a 45° angle back to horizontal polarization to avoid large power loss. Changing from Figure 15 to Figure 18 has minor improvements. Figure 18 roughly includes 4 prominent peaks" at 40°, 130°, 220°, and 310° as well as an additional 4 peaks at half of the height of prominent ones in between. Notably, the difference between the maximum and minimum Kerr Effect rotation is several times larger with this adjustment. Figure 19 that plots the signal power versus pump power is generally more linear than the previous measurement, excluding the drop in signal power between 350mW and 400mW of pump power.

Another set of data was collected where the power meter was measured the pump power reflected off the long pass BS placed after the Kerr Fiber. This was done after noticing that the data at certain intermediate pump powers was influenced by the previous power level, which is called hysteresis. Blocking the pump with the power meter to make measurements was possibly influencing the signal data received, as shown through the jump at certain pump powers in figure 15. Moving the power meter position allowed for the measurement to be made without blocking the pump beam. For Figure 15, data was collected from minimum power to maximum power as well as the reverse (maximum power to minimum power).

Figure 1 shows that theoretically ~648 microwatts would be required to maximize the signal pulse power. With 42% pump power coupling, a maximum of 850mW pump power, the 13.3mW total signal power, and assuming all of the coupled light is in the fundamental mode, the Kerr shutter would ideally measure 7.72mW of transmitted signal power. Since the measured value in these conditions was 31.7 μW, the shutter under the full fundamental mode coupling assumption has 0.41% efficiency. This assumption is faulty, as there's evidence of mode dispersion within the relative time pulse measurements in figures 5, 6, 7, and 8. Since the pump pulse dispersion is relatively even, a new assumption could be made that the pump has even mode distribution. Even mode distributions results in a division of the total power, which lowers the phase shift and thus shuttering capabilities. With 42% pump power coupling, a maximum of 850mW pump power, the 13.3mW total signal power, and assuming even power distribution between 10 pump modes, the Kerr shuter would ideally measure 0.0995mW of transmitted signal power. Since the measured value in these conditions was 31.7 μW, the shutter under the even power distribution among 10 modes assumption has 31.9% efficiency. Following the second calculation, the Kerr shutter has significant shuttering and should roughly follow the

characteristic equation of the sinusoidal squared function. This is roughly seen in figures 12 and 13 with a initial quadratic growth that tapers off. Maximum power levels allowed by the laser limited measuring a whole phase cycle by power.

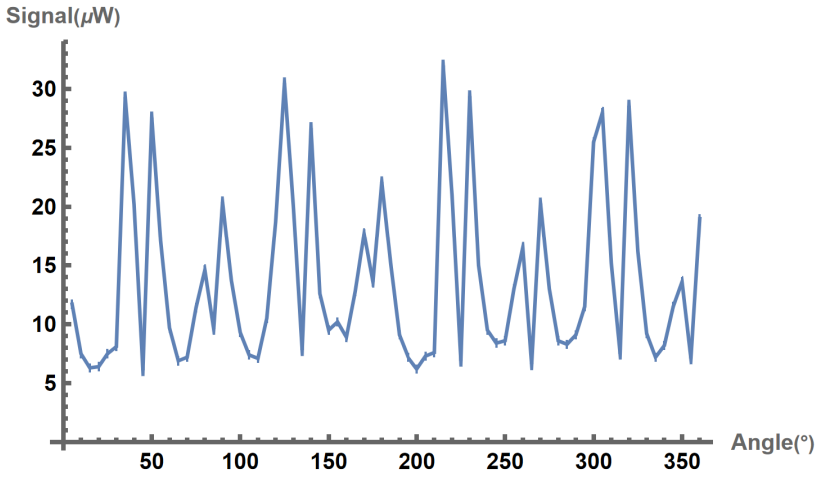

Figure 13: Signal Power (μW) vs. Pump HWP (°)

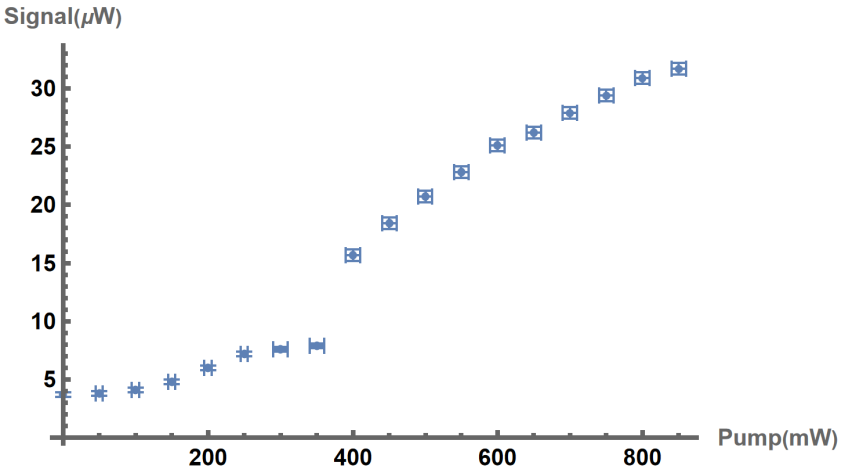

Figure 14: Signal Power (μW) vs. Pump HWP (mW)

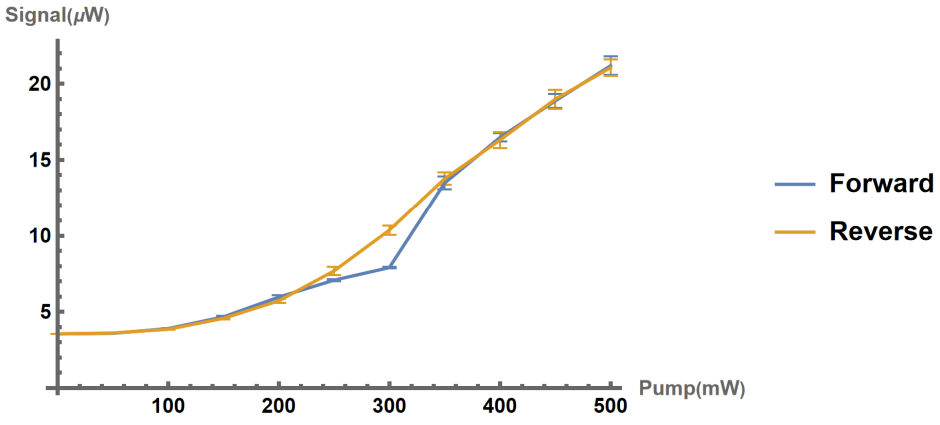

Figure 15: Signal Power (μW) vs. Pump Power (mW)

Raman Scattering

1550nm Raman scattering photon counts per second for varying pump pulse powers is plotted in figure 17. Before adding the 1550 bandpass filter, measurements were made of the Raman scattering with just the 1200nm long pass filter, so for photons >1200nm the Raman scattering for photon counts per second for varying pump pulse powers is plotted in figure 16. The Raman scattering photon counts per second are calculated as the mean counts from ten one-second trials at a given power subtracted with the mean counts for ten one-second trials of background measurements. The error for each point was calculated using Poisson statistics as the average of the square root of each number of counts per second.

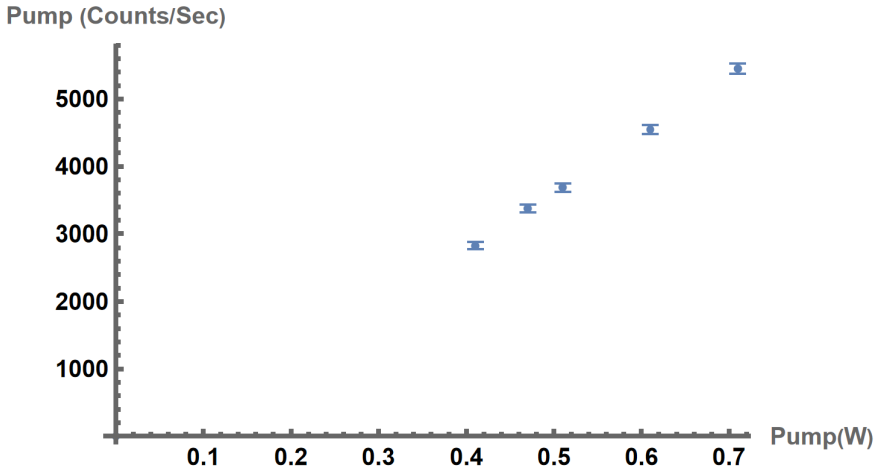

Figure 16: >1200nm Pump (Counts/Sec) vs. Pump Power(W)

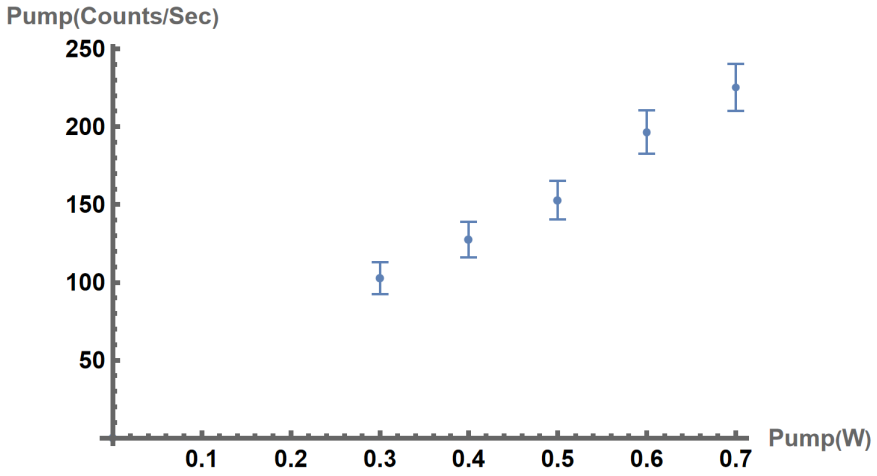

Figure 17: 1550nm Pump (Counts/Sec) vs. Pump Power (W)

DISCUSSION & CONCLUSION

Returning to the three driving questions of this research:

1. how can a Kerr-effect shutter with a 1550nm signal pulse and 850nm pump pulse be created to isolate two signal pulses separated by 200 picoseconds?
2. What impact will Raman Scattering from the pump pulse have on the signal pulse exiting the shutter?
3. Can the shutter be adjusted to function with single 1550nm photon pulses?

The project advanced far enough to begin addressing questions 1 and 2, but not 3, as answering question 3 requires understanding the first two well. The shutter cannot be adjusted to the single photon level if the background Raman scattering information must be remeasured and the Kerr effect measurements are weak.

Kerr Effect

The purpose of this research is to create a low-noise Kerr effect shutter. Let's first discuss whether a Kerr effect shutter was made. Analyzing each measurement, including the signal blocking, the signal to pump power relation, and the signal power to pump HWP angle, informs the extent to which the Kerr effect is observed. The pump pulse was verified to not be measured as transmitted signal power since the sensor zeros whenever the pump power was on, and the signal power was removed. The relation between signal and pump power was roughly quadratic, which follows what is expected from the small angle approximation. There are also nonlinear jumps at powers of around 300mW that are not well understood. These jumps may indicate hysteresis as shown in figure 16. Such jumps are also present in the relation between the signal power and pump half WP angle. After placing the isolator and an additional HWP to linearize

the pump pulses' polarization, the four expected prominent peaks spaced 90° apart were observed. However, all the measurements included 8 total peak clumps, with the adjustment resulting in shrinking four of these peak clumps. The both the presence of the 4 additional peaks as well as the peaks being unstable rather than smooth do not follow the expected behavior of a Kerr effect shutter and are not well understood. When measuring a signal power jump as a function of angles, a similar hysteresis phenomenon could be observed. When starting low the transmitted signal power would increase slowly and then suddenly jump. When reversing the angular direction, the signal power would decrease more smoothly. The mechanism causing these jumps is not well understood.

Measurements of the signal pulse were significant, though not efficient as 31.9% of the expected power was found. Possible factors causing lower efficiency and non-characteristic polarization rotation measurements are dirty optical components and pump pulses' mode distribution in the fiber. The HWPs on the pump optical path seem to be a bit dirty, which could change the polarization of the beam. Although equipment was inspected and cleaned before installation, dust naturally settles on optical equipment within the lab must be routinely verified. Additionally, a lot of power was focused into the Kerr fiber, so it should be inspected with a fiber microscope to not be burnt or damaged. Therefore, cleaning or switching out the HWPs, inspecting cleanliness of other optical components, and verifying the fiber ends are simple future tasks of this project.

While the fiber is single mode for the 1550nm signal pulse, it is multimode for the 850nm pump pulse. The phase shift equation was derived assuming the pump and signal to be in the fundamental mode. Therefore, the influence of non-fundamental pump modes overlapped with the fundamental signal mode was not accounted for. While the lens selection aimed to maximize

the amount of the pump pulse launched in the 1st mode to maximize overlap with the signal pulse, the pump pulse timing dispersion demonstrates that the pump was distributed in several modes. A meter long fiber was used instead of the initial 10cm fiber due to the fiber requiring polishing. The meter long fiber had to be coiled up, which can result in modes coupling together as the pulse travels. Both factors interfere with the simplified theoretical model. A future task of this research will be to replace the meter long fiber with a shorter fiber that can be extended straight out to avoid launching the pump into different modes as well as generally increase coupling efficiency. A few minor changes for the project moving forward are to readjust the signal pulse to not be on a mirror edge that adds error to the beam polarization as well as collect more data on the hysteresis of the Kerr effect. Cumulatively, the data indicates that certain aspects of the Kerr effect are present, but that there must be more adjustments to have a certain and efficient Kerr shutter.

Raman Scattering

Beyond measuring the presence of the Kerr effect, the research simultaneously attempted to complete initial measurements for the shutter to function in low noise regimes. Figures 16 and 17 follow the expected linear increase of Raman scattering as a function of pump power. A major limitation to these measurements is the possibility of having lost mode locking during the measurements. It was discovered after taking the measurements that there was pump pulse back reflection that would remove the mode lock when the pump power was above a few milliwatts. An isolator was added before taking the Kerr effect measurements to remove this issue and allow for higher pump powers to be used while maintaining the mode lock. While mode locking was done initially for the Raman Scattering, there were no checks to make sure that the pump

remained mode locked throughout the experiment. If the data was collected for CW pump then the measured Raman scattering power could be lower than if it were pulsed.[17] While the data provides a promising start to building a low-noise ultrafast Kerr effect shutter, the measurements must be redone with verified mode locking.

Summary

This research created the initial setup for what may eventually be a low noise ultrafast Kerr effect shutter as was aimed for by the three driving questions. Significant progress was made observing Kerr effect phase change with around 31.9% of the expected shift. Measurements of the transmitted signal power in relation to the pump polarization rotation and power resulted in finding mild supportive evidence as well as unexpected hysteresis properties. Next steps could include straightening the fiber to have a more stable modal distribution as well as cleaning optical equipment. Lastly, the Raman scattering measurements were initially promising but must be remeasured due to concerns over the pump pulse not being mode locked.

APPENDIX

Lens Selection

Coupling two laser beams with different wavelengths into the same optical fiber presents another challenge. Placing the beams onto the same optical path requires using a long pass dichroic beam splitter that reflects wavelengths below a cutoff and transmits wavelengths above the cutoff. Lenses are used to focus light into optical fibers. Chromatic aberration, which describes the extent that different wavelengths have different focal lengths, becomes a challenge for coupling two different wavelengths. An achromatic lens is used to have minimal focal distances between the two wavelengths and, therefore, help coupling efficiency. The pump pulse beam was profiled using photos and some analysis to check for an elliptical shape that could impact the coupling efficiency. The 1550nm single mode fiber used as the Kerr-effect medium has a mode field diameter of 10.4 microns. This small fiber diameter means that a small variation in focal point could lead to a much lower coupling efficiency. A Mathematica code was made to optimize the right focal point, focal point offset between the two wavelengths, and distance from beam waist that a lens would need to maximize coupling of 850nm and 1550nm laser pulses into the Kerr-effect fiber. 9mm focal point lenses with 2% error were selected as falling within an acceptable range of ~70% max theoretical coupling for the 850 beam that is not fully in focus.

Pump Beam Profiling

Beam characterization is another point of analysis. Laser beams typically have a circular gaussian spatial distribution perpendicular to beam propagation. Pictures on a MT9M001 ½ Inch Megapixel CMOS Digital Image Sensor were taken of the beam at various distances to calculate

how the beam diameter changes over propagation. This was completed using Mathematica by finding the gaussian best fit over the picture values.

Figures 18 and 19 show the close matching of the gaussian best fit to the values found from the photograph closest to the laser emitter. Figure 20 shows the X and Y radii profiling of the pump beam. Figures 18, 19, and 20 show that the Y axes radii is expanding more rapidly than the X axes radii. The original point of measurement had a circular beam while further out has an elliptical form. Given that optical fibers are cylindrical, having an elliptical beam will lower the coupling rate. This is an important feature to note given that the experimentally found coupling was much lower than expected.

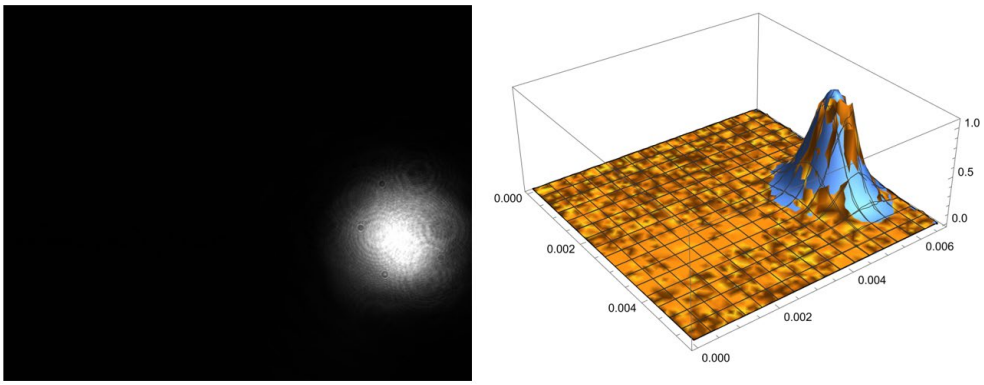

Figure 18: Photo and Distribution Fit of Pump Beam 1.04m from Laser Exit

Photo on the left. Gaussian fit made in Mathematica and plotted on meter scale on the right.

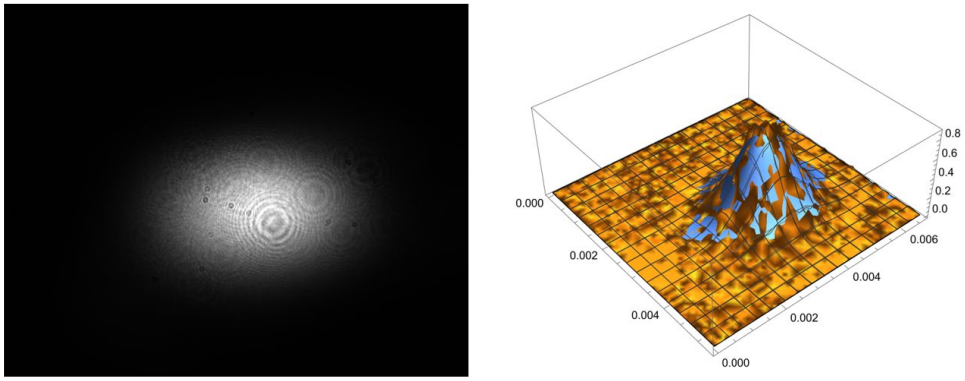

Figure 19: Photo and Distribution Fit of Pump Beam 2.54m from Laser Exit

Photo on the left. Gaussian fit made in Mathematica and plotted on meter scale on the right.

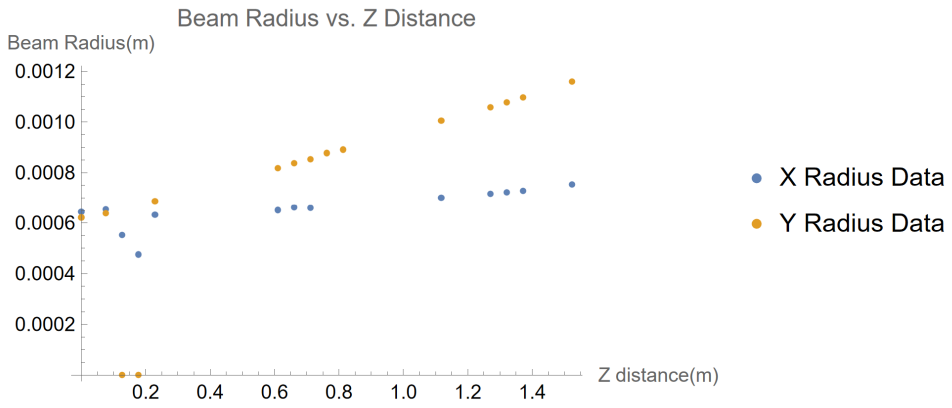

Figure 20: Pump Beam Profiling

Linear fit to points. Anomalies for a few data points within fitting process.

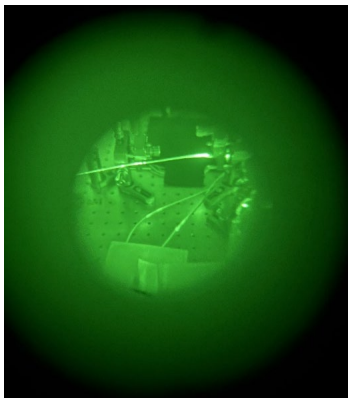

Figure 21: Photo of Infrared Light Leakage from Fiber

Bright spot is the entrance of the fiber. This means there's significant power loss upon coupling

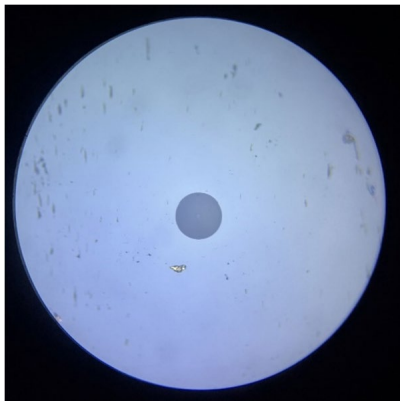

Figure 22: Microscope photo of Kerr Fiber End

Center small grey dot is the fiber core, the dark blue circle is cladding, and light blue is coating

Beam Coupling

High power is required from the 850nm pump beam to create enough birefringence within the fiber to significantly rotate a 1550 beam. Thus, high coupling of the 850nm beam into the Kerr fiber is needed to ensure lab safety as well as shutter power efficiency. Light that is not coupled can be reflected in unpredictable ways that, at high power, can become a safety concern for researchers in the lab. There are numerous possible reasons why found coupling of the 850nm beam is at maximum 70% compared to the expected near 100%. One explanation is that there's significant light leaks from within the Kerr Fiber, as shown in figure 21 with a photo from an infrared viewer. Another explanation for the low coupling rate is physical issues within the fiber. This can be caused by having a dirty fiber end which light reflects off or internal fiber damage. Fibers are routinely cleaned before reconnecting them, but this is not completely full proof. Figure 22 shows the end of the optical fiber used, with clean core and cladding but dirty coating. The chances of internal fiber damage are low since an IR viewer would immediately detect the higher reflectivity in that section. The coupling of the 1550nm beam out of the Kerr fiber into the 1550nm detector reaches up to 80%, which is typical.

BIBLIOGRAPHY

1. Yabuno, M. *et al.* Ultrafast measurement of a single-photon wave packet using an optical Kerr gate. *Opt Express* **30**, 4999–5007 (2022).

2. Cameron, A. *et al.* Ultrafast Measurement of Energy-Time Entanglement with an Optical Kerr Shutter. (2023).

3. Fuller, P. An introduction to high speed photography and photonics. *Taylor Francis* **57**, 293–302 (2009).

4. Nozaki, K. & Tanabe, T. Sub-femtojoule all-optical switching using a photonic-crystal nanocavity. *Nat. Photonics* (2009) doi:https://doi.org/10.1038/nphoton.2010.89.

5. Clegg, B. *The Man Who Stopped Time: The Illuminating Story of Eadweard Muybridge?: Pioneer Photographer, Father of the Motion Picture, Murderer*. (Joseph Henry Press, 2007).

6. The Nobel Prize in Physics 2023.

7. Mikami, H., Gao, L. & Goda, K. Ultrafast optical imaging technology: principles and applications of emerging methods. *Nanophotonics* **5**, 497–509 (2016).

8. Visible Light. *NASA* https://science.nasa.gov/ems/09_visiblelight/.

9. Saleh, B. & Teich, M. *Introduction to Photonics*. (Wiley Interscience, 2007).

10. Griffiths, D. J. *Introduction to Electrodynamics*. (Pearson Education, 2014).

11. Friberg, S. & Smith, P. Nonlinear optical glasses for ultrafast optical switches. *IEEE J. Quantum Electron.* **23**, 2089–2094 (1987).

12. Agrawal, G. P. *Applications of Nonlinear Fiber Optics*. (Academic Press).

13. Kupchak, C., Erskine, J., England, D. & Sussman, B. Terahertz-bandwidth switching of heralded single photons. *Opt Lett* **44**, 1427–1430 (2019).

14. Li, J. & Zhang, M. Physics and applications of Raman distributed optical fiber sensing. *Light Sci. Appl.* **11**, (2022).

15. Raman, C. & Krishnan, K. A New Type of Secondary Radiation. *Nature* (1928) doi:https://doi.org/10.1038/121501c0.

16. Sirleto, L. & Ferrara, M. Fiber Amplifiers and Fiber Lasers Based on Stimulated Raman Scattering: A Review. (2020).

17. Hu, C.-R. *et al.* Stimulated Raman scattering imaging by continuous-wave laser excitation. *Opt Lett* **38**, 1479–1481 (2013).